Brazilian Journal of Geophysics 42 (2024), 3, 1-15
Brazilian Geophysical Society
ISSN 2764-8044
DOI: 10.22564/brjg.v42i3.2326

PORE TYPE AND ASPECT RATIO PREDICTION - A KNOWN PARAMETER FOR SEISMIC MONITORING STRATEGIES - AND THE PRE-SALT RESERVOIR CARBONATIC ROCKS APPLICATION

Evângela P.A. da Silva[1], Alessandra Davolio[2], Marcos Sebastião dos Santos[2], and Denis J. Schiozer[2]

[1] Petrobras, Santos, SP, Brazil
[2]Unicamp, CEPETRO, Campinas, SP

* Corresponding author email: evangela@petrobras.com.br

ABSTRACT. Microbialites and coquinas compose the large pre-salt carbonate reservoirs for hydrocarbon accumulations of the Santos Basin, Brazilian offshore. The complexity of this type of rock poses major challenges for the reservoir characterization, especially the microbialites ones. This article presents a well log study relating the deviations of P-wave velocities with the aspect ratio observed in these specific rocks. In our suggested approach, we analyze the facies logs to obtain a relation between these deviation effects and the pore type. The facies analysis allows us to better separate the microbialite and coquina rocks, covering significant differences in porosity and diagenetic processes. We state for the analyzed rocks that the vug features are the predominant pore type for both lithologies, and that this aspect reflects the results of velocity deviations and aspect ratio values. This information is applied to build petro-elastic modeling to assist in seismic monitoring of the reservoir.

Keywords: P-wave velocity deviations; petro-elastic model

INTRODUCTION

Currently the pre-salt reservoir in the Santos Basin plays as one of major global exploration and production targets of the last decade. The increasing of systematic study related to this reservoir happens after the conclusion of the first well focusing on that objective (Well 1-BRSA-329D-RJS, called Parati prospect in Block BM-S-10, concluded in 2005). Even not being a commercial well it has spurred oil and gas exploration until the Tupi discovery, wich started its production in 2009 (Maul *et al.*, 2021). Since than several new fields were discovered in the Santos Basin, and the producing rock formation are Barra Velha and Itapema formations. Microbiolites and coquinas are the main carbonate facies found in these formations (Moreira *et al.*, 2007).

The petro-elastic models´ construction requires knowledge of the properties of the rocks´ pore structure, which mainly depend on the morphology pore space and solid phases of rock. The modeling of carbonate reservoirs is more complex than that of siliciclastic, due to their distinctions, such as mineralogical composition, environments depositional aspect, diagenetic processes, internal porous structure. Methodologies efficient in the siliciclastic rocks

most of the time have deficientness for carbonatic rocks. While the former of siliciclastic ones have mostly ellipsoidal pores (intergranular), the carbonatic have pores ranging from rounded, ellipsoidal to elongated. Therefore, the porous geometry has strong influence on carbonates' rock physics, imposing important variation for the intrinsically porosity (Mavko *et al.*, 2009).

Choquette & Pray (1970) divide pore type in carbonatic rocks into 15 classes, following different aspects of genetical or physical. Because these pore´s complexities are controlled by diagenetic processes and they give clues about permeability, the pore structure prediction can give to us a very insightful information about the reservoir characteristic (Harahap *et al.*, 2020).

According to Saberi (2013), the science of rock physics creates a link between elastic properties (e.g. P-velocity/S-velocity ratio, elastic modulus), reservoir properties (e.g. porosity, saturation, pressure) and reservoir architecture (e.g. lamination, and fracture). The pore type complexity in carbonate rocks, previously mentioned, affects the seismic primary velocity up to 40% (Xu & Payne, 2009). This complexity gives implications to cross-plot scattering in porosity-velocity relationship for the carbonatic rocks.

Anselmetti & Eberli (1993, 1996, 1999) demonstrate that the main variations in the geometry of the pore space in carbonates influence the acoustic velocity, confirming a strong dependence with the combination porosity factors and pore structures. As per the author conclusions, starting from an initial defined velocity, we can observe that: i) positive velocity deviations (above +500 m/s): indicate high velocities related to the porosity, with pores of the intrafossil or moldy type; ii) moldy porosity would be indicative of intense diagenetic changes, favoring the reprecipitation of minerals and cementation of pores and it is characterized by pores commonly not connected, with a dense cemented matrix, being indicative of low permeabilities; iii) deviations close to zero (±500 m/s or less) indicate low velocities and porosity of interparticle type, intercrystalline or microporosity, specially, associated with few diagenetic changes, prevailing pores typical of the post-sedimentation process, where the original grains or micrites are packaged together. The aspect is characterized by pores usually well connected producing high permeability, except when only the microporosity is abundant; and iv) negative deviations (below -500m/s), that can be caused by the presence of fractures and gas, excluding the other factors that can also cause low velocities such as well wall problems.

In this work we applied the method proposed by Anselmetti & Eberli (1993, 1997, 1999) to define the aspect ratio of rock appearance by range of velocity deviations P, to be included in the model proposed by Xu & Payne (2009).

In this way, using the information of one well that reaches the pre-salt reservoir in the Santos Basin as our material of study, we consider the pore geometry influence in the petro-elastic model for carbonatic rocks affecting the seismic velocity in a different manner, because we assume that for the same porosity value the velocity can be higher or lower depending on the pore type (Castro & Rocha, 2013; Harahap *et al.*, 2020; Silva *et al.*, 2020).

Analysis of the facies log

To assist in the results interpretation that were obtained by applying the method mentioned before, the facies created in the well were used, after facies calibration, considering the description of samples sides.

The facies logs corresponding to a combination of lithology, type of pores, porosity and diagenetic process, and their respective proportions are shown in Figures 1, 2, 3 and 4, in which the zones corresponding to microbialite and coquina are identified (adapted from Silva *et al.*, 2017).

In Figure 1, we present the lithological facies log, along with graphs of the percentage of these compositions, in addition to three thin sections exemplifying the main lithological types observed in the log. According to the description of the lithofacies log (Fig. 1), the microbialite zone is composed of: spherulite (33%), laminite (12%), stromatolite (5%), by associationamoongspherulite/laminate (27%) laminite/spherulite/stromatolite (18%); mudstone (3%) and wackstone (2%), not very representative. The coquina range is basically composed of coquina (95%). Figure 1 shows that microbialite is more heterogeneous than coquina, with a predominance of laminites and spherulites in its lithology.

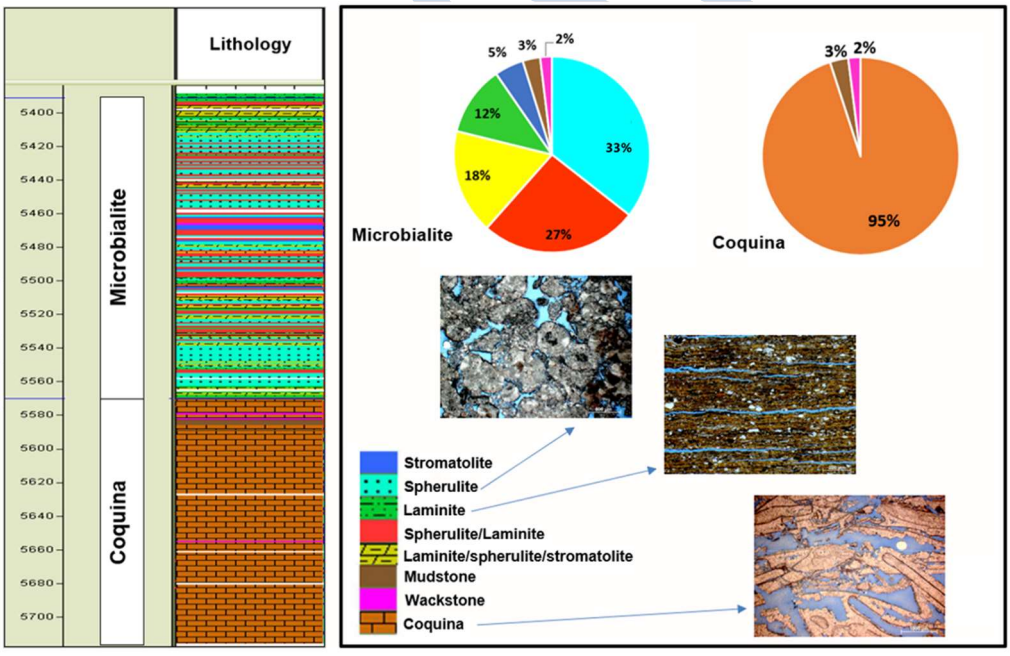

Figure 1: Facies log of lithology showing microbialite and coquina composition in the studied well. Note the predominance of laminite and spherulite in the microbialite. Adapted from (Silva *et al.*, 2017).

In Figure 2, the porosity log is added next to the lithological facies log, and we present the graphs in percentage with the main porosities observed in microbialite and coquina. It is worth mentioning that this is a macroscopic classification of porosity. As shown by the facies log of porosity (Fig. 2), the best values are found in the coquina interval, in which we interpret mostly as good (48%) and reduced (30%) porosities, while in the most of the microbialite we classify the porosity as closed (74%) or reduced (22%).

In Figure 3, in addition to the facies and porosity logs, we show the diagenetic process log along with graphs emphasizing the predominant type of the two zones, microbialite and coquina. Its analysis shows that the porosity seems to be related to the diagenetic process described in the well. It is possible to observe in the process facies log, that the dolomitization was the main diagenetic process in the microbialite with occurrence corresponding to ~65%; when dolomitization is associated with silicification corresponding to 27%; and the silicification occurs in 8% of the rocks. In 6% of the samples did not observe any process.

In coquina, the main diagenetic process (Fig. 3) was recrystallization, which is present in almost the entire range. However, only 6% of the rocks occur in an isolated manner. The biggest occurrences correspond to the association of recrystallization with dolomitization (37%); dolomitization and silicification (35%); and with silicification only (7%), with lower expression.

The dolomitization and silicification process were described in some portions of the log corresponding to, respectively, 10% and 1.5% of the occurrence in this interval, when both processes are present correspond to 3.5%.

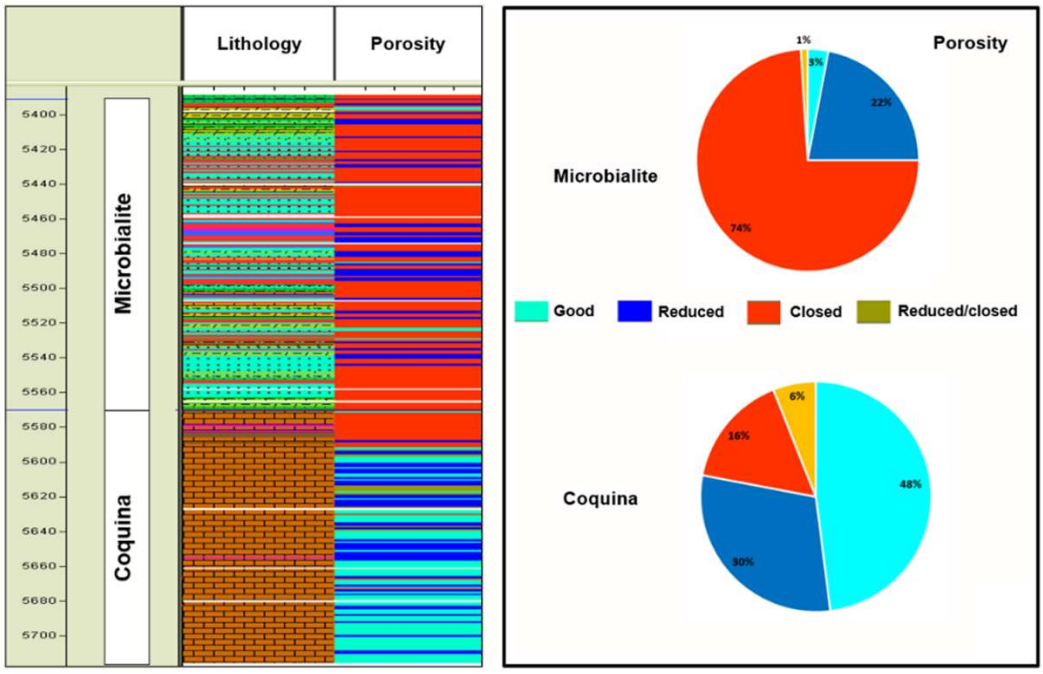

Figure 2 – Porosity log next to the facies log. The proportion of porosities can be compared between microbialite and coquina, in which coquina is observed to be more porous. Adapted from Silva et al., (2017).

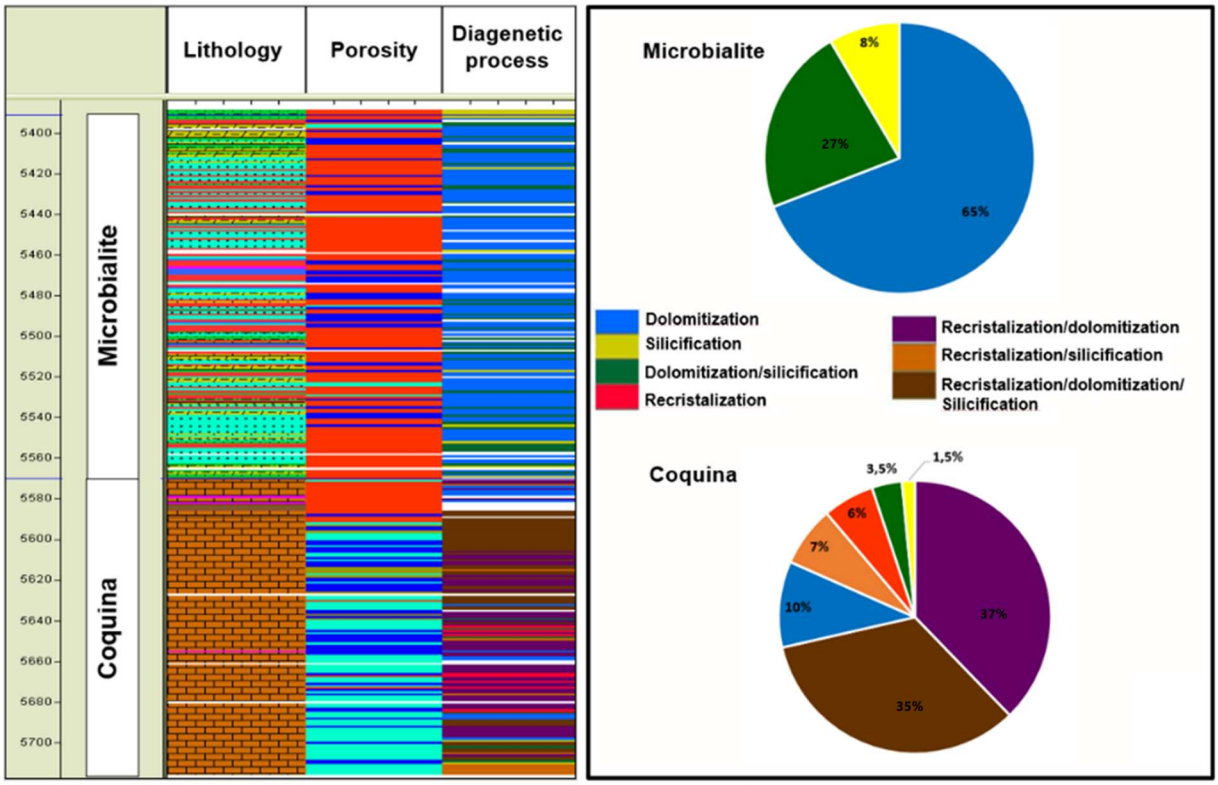

Figure 3 – Diagenetic process logs next to the facies and porosity logs. It is observed that dolomitization was the dominant process in microbialite, while in coquina it is combined with the recrystallization process. Adapted from Silva et al., (2017).

In Figure 4, the pore type log is added to the other ones (lithological, porosity and diagenetic processes), together with graphs of percentage of their occurrence by zone, and thin sections exemplifying some types of porosity observed in carbonatic rocks.

The types of pores we show in Figure 4 emphasize how predominant the vugs are in microbialites, corresponding to approximately 86% of the range; other types of pores also occur in association with vugs (minor occurrences) and they are: framework (6%), fenestral (5%) and intercrystalline (~1.3%). When not associated with vugs, the fenestral porosity type and framework represent less than 3% of the range. In coquina, as in microbialite, the predominant type of pores are the vugs (45%), which can occur in association with moldy and intercrystalline porosity (31%), or only moldy (16%) or intercrystalline (6%). It may also be associated with moldy and intergranular (1.5%). The fenestral porosity corresponds to 0.5% representation.

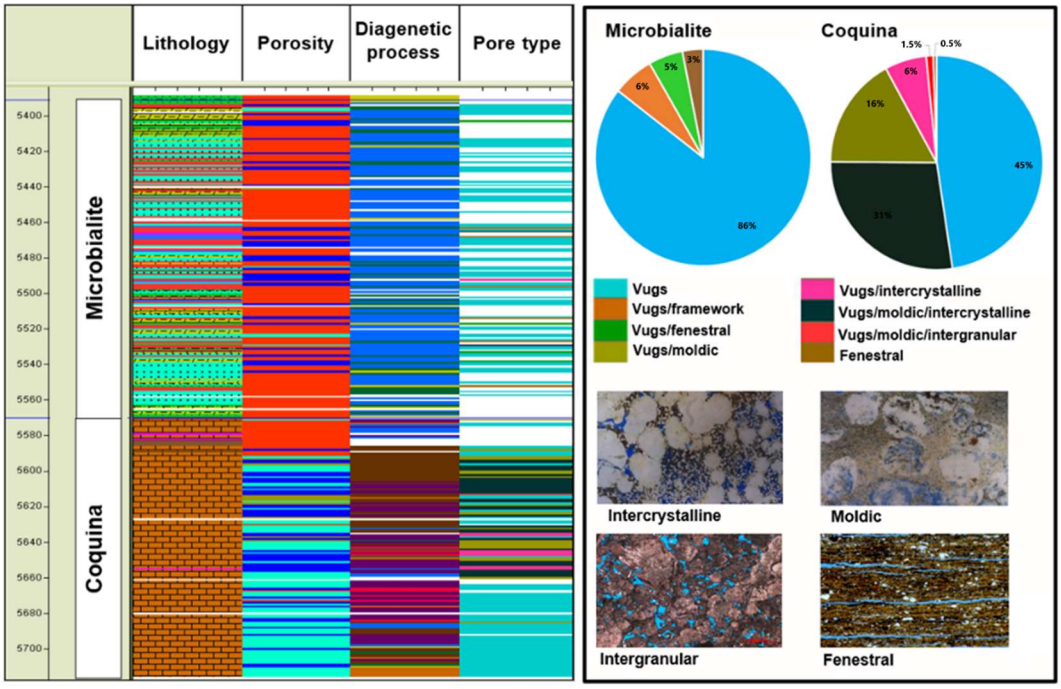

Figure 4 – Pore type log next to the facies, porosity, and diagenetic process log. Note in the pore type proportion graph and in its log that the vugs type is predominant in microbialite and coquina. Adapted from Silva et al.,(2017).

The facies analysis performed from the description of lateral samples in the well shows the separation between microbialite and coquina. Given the lithological differences, we analyzed the diagenetic process described in the log samples, in which we observe that the dolomitization, whether associated with silicification, predominates in the microbialite facies; while in coquina facies the recrystallization, in association or not with dolomitization and silicification, was the dominant process. In the coquinas we noticed the best porosities compared with the microbialite occurrences, which often presents closed and/or reduced porosity. Finally, the vug pore type is predominant in both intervals, and in coquina they are mainly associated with moldy, interparticle and intercrystalline porosity..

GEOLOGICAL SETTING

The Santos Basin is the largest basin along the Brazilian coast, covering an area of about 350.000 km^2. As per Garcia *et al.* (2012), the basin is limited in the NE by the Cabo Frio High and the in the South for the Florianopolis High (Fig. 5). Its origin begins in the Cretaceous with the breakup of the supercontinent Gondwana, with the opening of the South Atlantic (Kukla *et al.*, 2018) and comprises four unconformity-bounded tectono sedimentary megasequences (Ponte and Asmus, 1978; Chang *et al.*, 1992): the continental rift stage with fluvial and lacustrine sediments dated as Late Jurassic–Early Cretaceous; the Aptian transitional evaporite stage; the Albian restricted marine carbonates; and the open-marine megasequence, dated from the Cenomanian to Present (Moreira *et al.*, 2007).

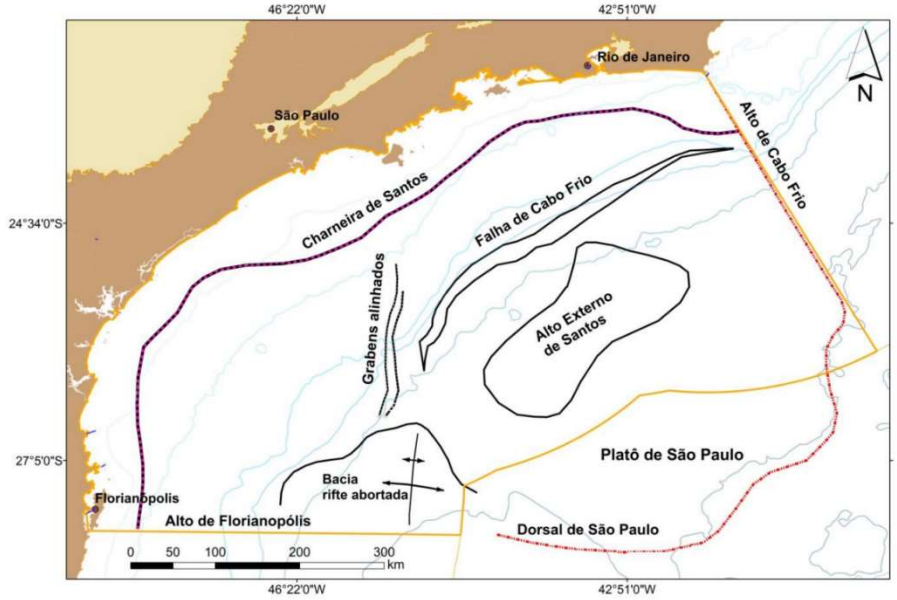

Figure 5 - Location and limits of the Santos Basin, Brazilian offshore. Adapted from Garcia et al. (2012).

The Early Aptian, named Itapema (ITP) and Barra Velha formations (BVE), which represent the main pre-salt reservoir rocks (Faria *et al.*, 2017), is the subject of this work. It was initially filled by lacustrine to restricted marine carbonates (Mann and Rigg, 2012; Quirk *et al.*, 2012) including coquinas, stromatolites, grainstones, laminites and spherulites. The current stratigraphy adopted for the Santos Basin (Fig. 6) generally mentions the rift, transitional (post-rift) and drift phases (Moreira *et al.*, 2007).

Lithostratigraphically, the Itapema Formation is at the top of the sedimentary section of the rift, being separated from the Barra Velha Formation by a regional unconformity (pre-Alagoas unconformity), which is at the base of the sedimentary section of the post-rift phase, (Moreira *et al.*, 2007).

The dataset used in this study contain one single well, provided by The Brazilian National Petroleum Agency (ANP), and it was chosen because it represents two distinct rock types, microbialite, with main occurrence in the Barra Velha Formation and coquina, present in the Itapema Formation. The reservoir, with excellent quality oil, are located about 300 km from the Brazilian coast, at total depths of approximately 5,000 meters, with 2,000 meters of water depths, 1,000 meters of mainly siliciclastic sediments and other 2,000 of evaporites (Petrobras website: https://petrobras.com.br/pt/nossas-atividades/principais-operacoes/bacias/bacia-de-santos.htm).

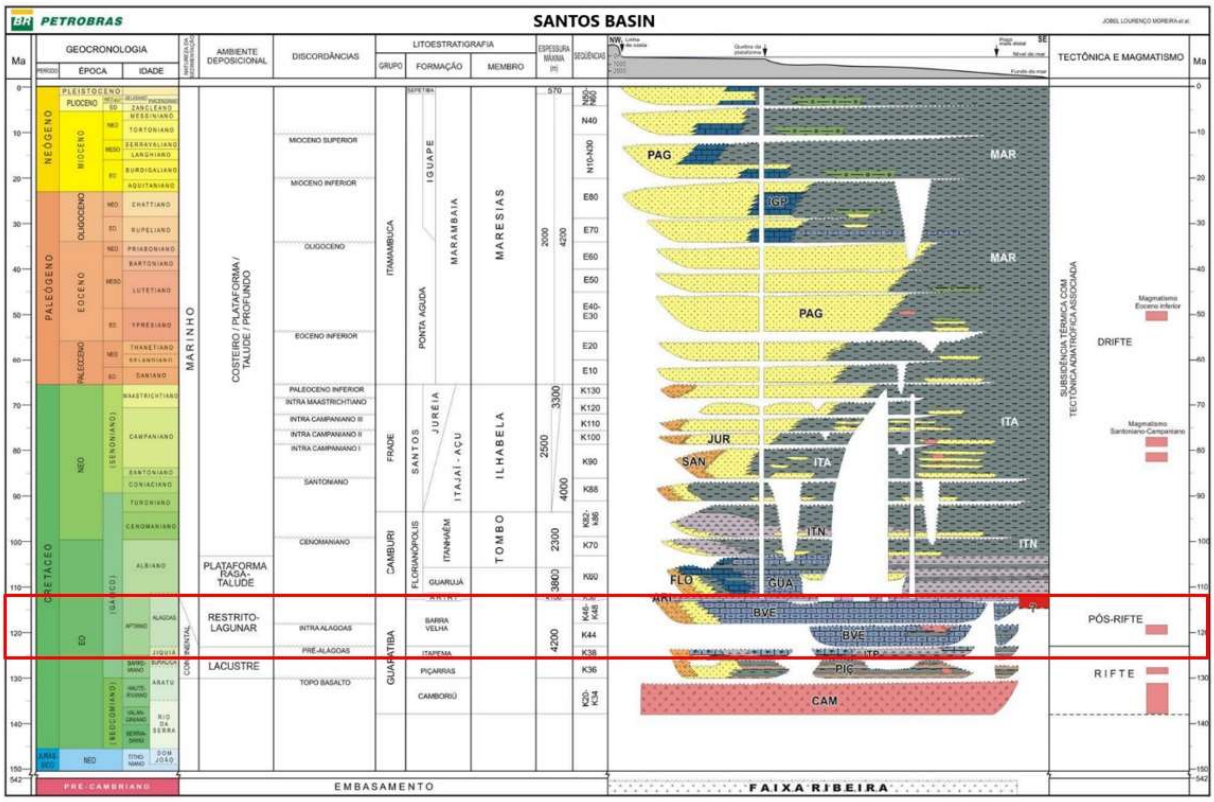

Figure 6 – Current Santos Basin stratigraphic chart illustrating the short period of deposition for the Itapema and Barra Velha formations. Adapted from Moreira et al. (2007).

METHODS

To obtain the P-velocity deviation logs we applied the method proposed by Anselmetti & Eberli (1999), in which new P-wave velocities obtained from the Willie´s equation (Wyllie *et al.*, 1956), and subtracted from the velocity calculated from the sonic log:

- Generation of three velocity deviation logs, considering the following input logs of porosity: NPHI (obtained from neutron porosity log), TCMR (obtained from the total porosity of the magnetic resonance log) and Por_RHO (obtained from porosity calculated with the density log).
- Analysis of the three velocity deviation logs to search for patterns allowing us to identify the different areas of interest; and later, to relate such deviations, graphically, with the aspect ratio of the rock.
- For a better understanding of the results obtained from the P-velocity deviations, we analyzed the logs of lithology, porosity, diagenetic process and pore type, based on the previous interpretation of the sides of the samples ANP has provided.

RESULTS, ANALYSIS AND DISCUSSON

Figure 7 shows the results we obtained for the P-wave velocity deviations, based on the NPHI, TCMR and Por_RHO, for the microbialite and coquina intervals, along with the water saturation (Sw) and silica volume (Vsi) logs in the well.

In Figure 8 the results of Pwave velocity deviations were placed next to the lithology, porosity, diagenetic processes and pore type logs, considering only the oil zone in the well. When analyzing the results of deviations from P-velocity (Figs 7 and 8), in terms of positive deviations and negative, it is observed that:

- Deviation from NPHI: microbialite shows pattern mostly positive, and in contrast, the coquina, in the zone of oil, a pattern is observed predominantly negative. In the water zone of coquina, the pattern of deviation intercalates between positive and negative (first part of the log) and negative in the second, in which the deviations from velocity seem to be influenced by the presence of silica (depth under 5850 m).
- Deviation from TCMR: The standard of deviation in the microbialite is positive; while in coquina it is observed that the deviations oscillate between positive and negative, with predominance of positive values, regardless of the fluid present in the rock (oil or water zone).
- Deviation from Por_RHO: in microbialite the default of deviation is both positive and negative, with the first half of the log more negative and the second positive; and in the coquina it shows predominantly positive.

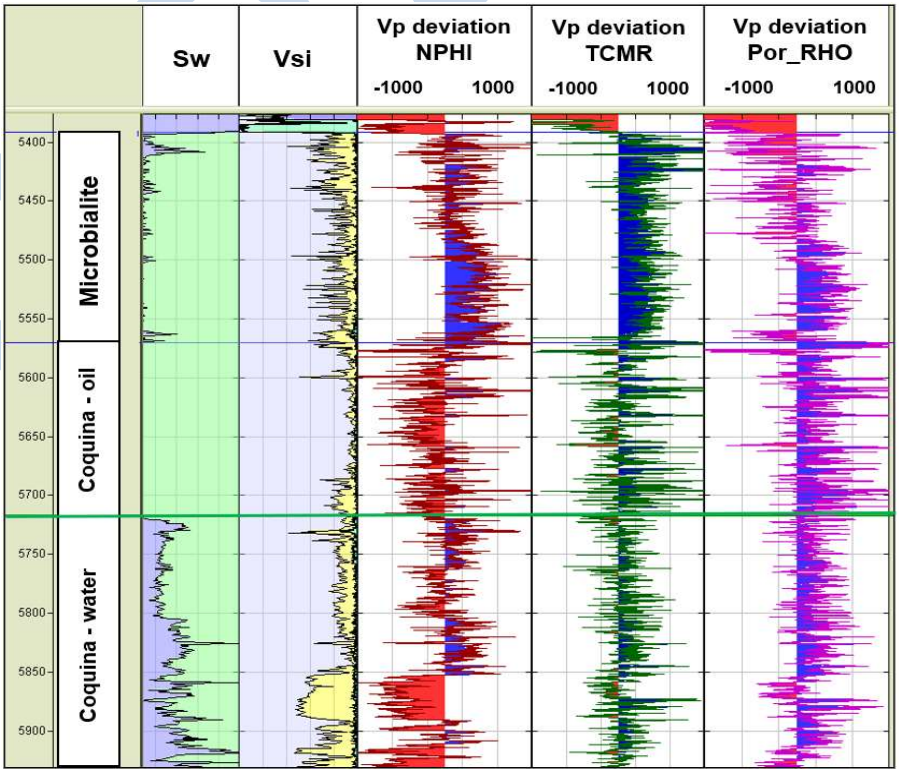

Figure 7 - Water saturation (Sw) logs (in faded blue), silica volume (Vsi) (in yellow) and velocity deviations of the P-wave of the three porosities: NPHI, TCMR and Por_RHO in the microbialite and in the coquina zone. The positive deviation is in blue hatch while the negative deviations are in red hatch.

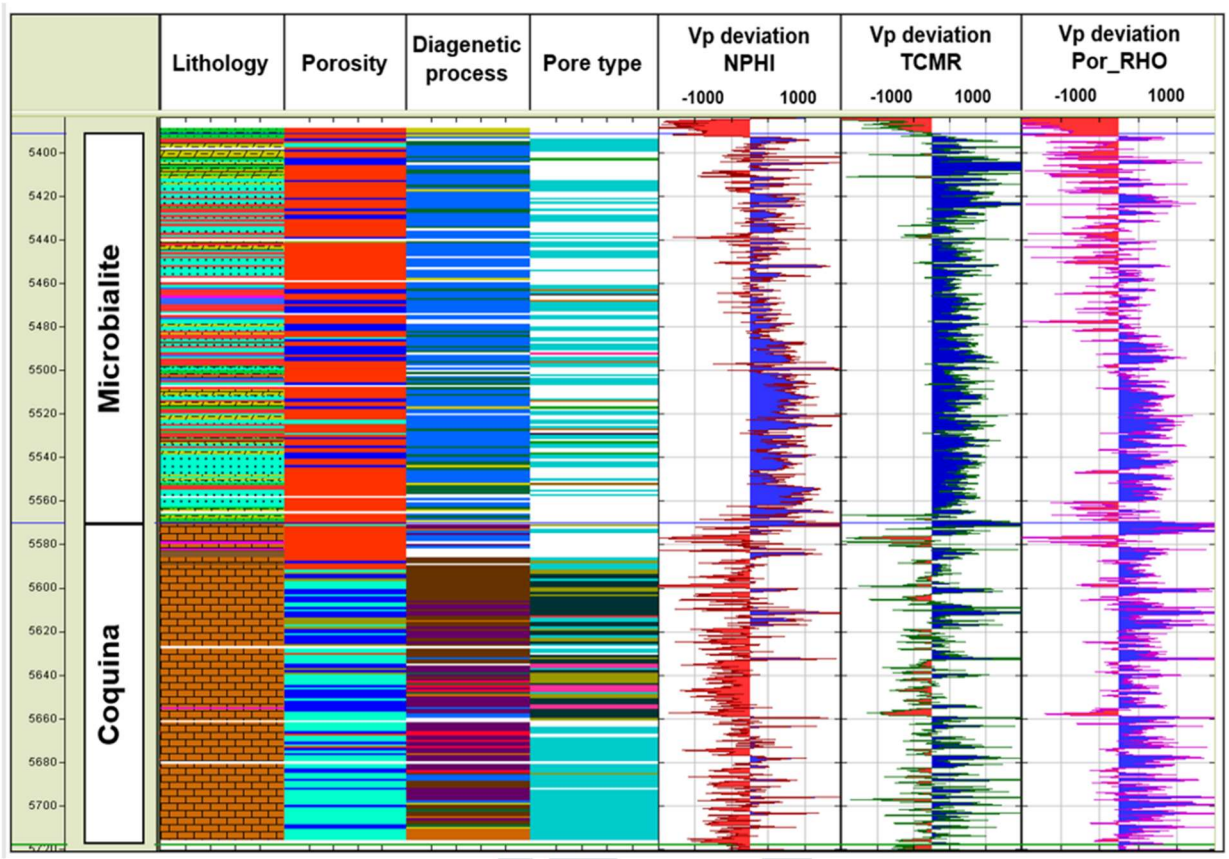

Figure 8 - Facies logs: lithology, porosity, diagenetic process and pore type; and deviations of the P-wave velocity of the three porosities: NPHI, TCMR and Por_RHO. The positive deviation is in blue hatch while the negative deviations are in red hatch.

Figures 9 and 10 show the P-wave velocity values as a function of porosity, colored by the P-velocity deviation, for microbialite and coquina, respectively. The aspect ratio values present variation between 0.01 and 0.5, in which the higher the value, the more rounded the pore.

The cross-plots of Porosity versus Vp (Figs 9 and 10), help to verify the relationship between the velocity deviations and aspect ratio of rock pores for microbialite and coquina. According to Anselmetti & Eberli (1999), deviation values above 500 m/s are reflections of intrafossil or moldy porosity. In the microbialite zone it is observed that the vug facies are those that presented such deviation values, or that is, above 500 m/s, which correspond to the aspect ratio above 0.16, regardless of the deviation curve of velocity used. In coquina it is verified that such deviations are associated with both vugs and moldy porosity, also corresponding to values of 0.16 of aspect ratio.

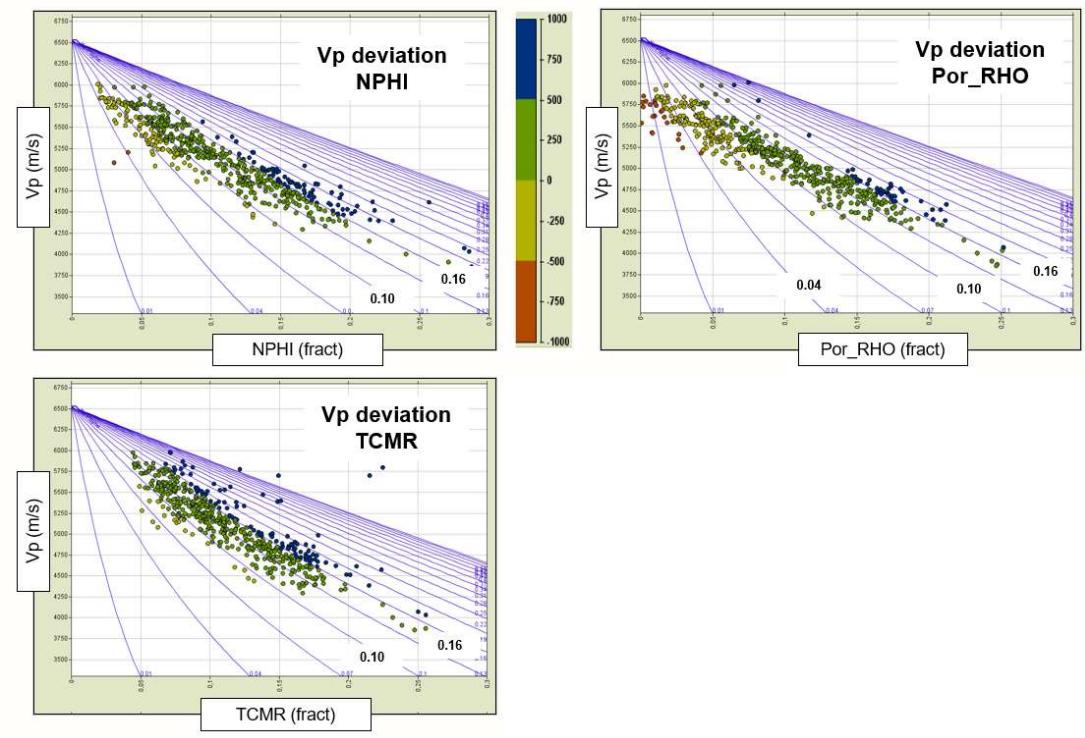

Figure 9 - Porosity x P-velocity, colored by the velocity deviation of the P-wave (m/s) of the three porosities (NPHI, TCMR and Por_RHO) for the microbialite. The aspect ratio values are informed by the blue lines in the cross-plot (variation between 0.01 and 0.5) in which the higher the value, the more rounded the pore. Deviations above 500 m/s are shown in blue; deviations of -500 m/s in red; and deviations between ±500 m/s were divided into green and yellow, to highlight positive and negative deviations, respectively.

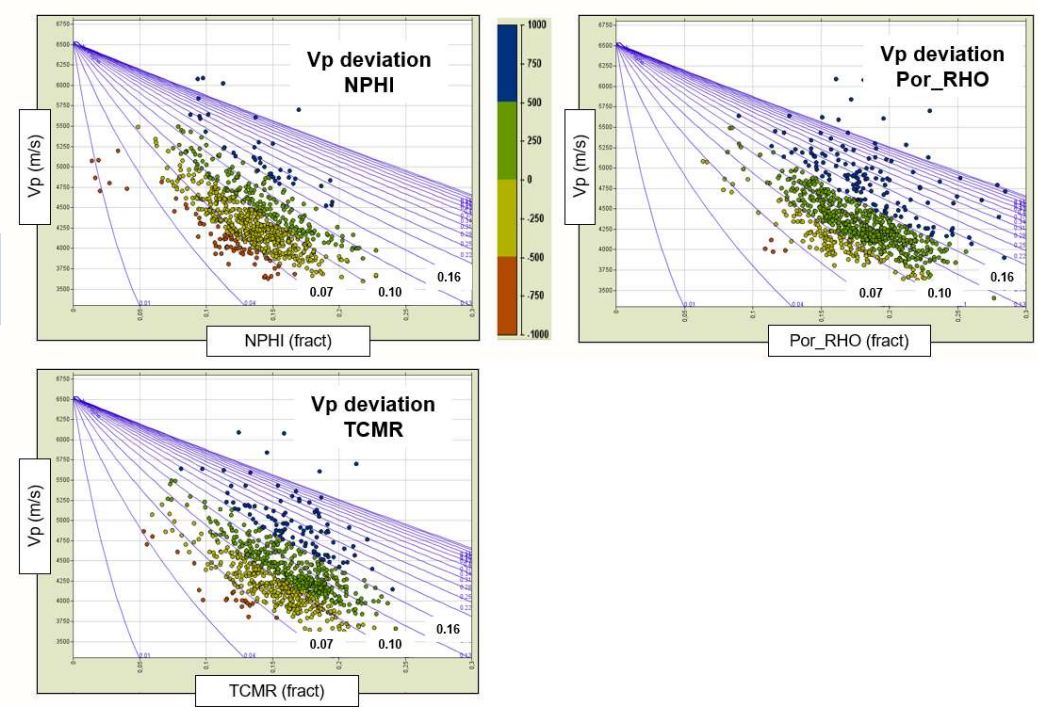

Figure 10 - Porosity x P-velocity, colored by the velocity deviation of the P-wave (m/s) of the three porosities (NPHI, TCMR and Por_RHO) for the coquina. The aspect ratio values are informed by the blue lines in the cross-plot (variation between 0.01 and 0.5) in which the higher the value, the more rounded the pore. Deviations above 500 m/s are shown in blue; deviations below -500 m/s in red; and deviations of ±500 m/s were divided into green and yellow, to highlight positive and negative deviations, respectively.

Velocity deviations of ±500 m/s (or less) occur due to the presence of interparticle porosity and intercrystalline, according to Anselmetti & Eberli (1999). The results obtained are mostly within their range of values, where the aspect ratio corresponding between 0.16 and 0.04, with exception for microbialite in Por_RHO deviation log; and for coquinas in the NPHI deviation log, whose velocities values above -1000 have an aspect ratio of 0.01.

Due to the difference in patterns of velocity deviations obtained in the TCMR log, in which the microbialite was well marked by positive values and the coquina by the oscillation between positive and negative for both the oil and water range, this log was chosen to define the aspect ratio along the well. Therefore, it is observed that the types of pores vugs and moldy are responsible for the deviation positive velocity, while those of the type interparticle and intercrystalline would be more associated with negative velocity deviations (Fig. 8).

Thus, as shown in Table 1, the aspect ratio that best describes the microbialite considering positive P-velocity deviations above 500 m/s is 0.19, corresponding to the proportion of 23% of the interval; for deviations of ±500 m/s we have founded an aspect ratio of 0.12 with proportion of 77%; deviations of less than -750 m/s were not observed. In coquina there is 0.22 corresponding to 13% proportion for deviations above 500 m/s; 0.13 with 84% proportion for deviations of ±500 m/s; and an aspect ratio of 0.05 with 3% for deviations less than -750 m/s.

Table 1 - Aspect ratio and its proportion corresponding to each velocity deviation interval of TCMR (m/s) for microbialite and coquina.

	Microbialite		Coquina	
P-deviation	**Aspect Ratio**	**Proportion**	**Aspect Ratio**	**Proportion**
Above 500 m/s	0.19	23%	0.22	13%
±500 m/s (or less)	0.12	77%	0.13	84%
Below -750 m/s	-	-	0.05	3%

According to Silva *et al.*, (2020), the values best fitting these well logs (P-velocity and S-velocity), obtained iteratively, correspond to the curve that considers the most extreme points of the cross-plots for P-velocity deviation for microbialite and coquina, and not to the curve that considered the midpoints (Tab. 2). Although discrepant, it is observed that: a) the highest frequency obtained for the aspect ratio values (α_2=0.18) represents velocity deviations values above 500 m/s (0.19), evidencing the predominance of vugs in the microbialite; and b) velocity deviation of ±500 m/s for the coquina, evidences the presence of vugs associated with the type of intercrystalline and interparticle pores, which is an aspect ratio value (α_2=0.15) close to that showed in the Table 1 (0.13). Another point to be considered is the fact that in the

modeling by Xu & Payne (2009), S-velocity also needs to be calibrated in addition to P-velocity, and it is necessary that the aspect ratio values, as well as their frequency of occurrence, are adequate for both seismic properties (P-velocity and S-velocity).

Table 2. Aspect ratio (α_1, α_2, and α_3) values and their respective frequency occurrences (F_1, F_2, and F_3) used in petro-elastic modeling based on Xu and Payne (2009) for microbialite and coquina (Silva et al., 2020)

Aspect ratio for microbialite and coquina zones						
Zone	***α_1***	***F_1 (%)***	***α_2***	***F_2 (%)***	***α_3***	***F_3 (%)***
Microbialite	0.35	20	0.18	75	0.07	5
Coquina	0.35	20	0.15	75	0.04	5

CONCLUSIONS

We show that it is effective to use known patterns of velocity deviations in relation to the pore types in predicting intervals of interest where there are no described samples.

Of the three velocity deviation curves analyzed, NPHI, TCMR and Por_RHO, the second was the one that best separated the microbialite facies from the coquina ones.

The pore type of vug is the predominant one in both intervals, being that in microbialite is more associated to intrafossil and moldy porosity and in the coquina, they are mainly associated to moldy porosity, interparticle and intercrystalline pores.

Considering the differences in deviations from P-velocity we state the aspect ratios are representative of the same intervals for the microbialite and coquina, showing very similar values.

The method is a good starting point to obtain aspect ratio values from P-velocity deviation prior to building petro-elastic models, to assist in seismic monitoring of the reservoir. However, some adjustments can be necessary, since the parameters must also fit in the calibration of S-velocity, in addition to P-velocity.

ACKNOWLEDGMENTS

This work was conducted with the support of Libra Consortium (Petrobras, Shell Brasil, Total Energies, CNOOC, CNPC), PPSA, and Energi Simulation within the ANP R&D levy as "commitment to research and development investments". The authors are grateful for the support of the Center for Petroleum Studies (CEPETRO-UNICAMP/Brazil), the Department of Energy (DE-FEM-UNICAMP/Brazil) and Research Group in Reservoir Simulation and Management (UNISIM-UNICAMP/Brazil). In addition, a special thanks to CMG, SLB, and CGG for software licenses. The authors would also like to thank the Petrobras Reservoir

Geophysics Management for their unlimited support of this work, especially Paulo Roberto Schroeder Johann and Rui Cesar Sansonowski, and the geophysicists Alexandre Rodrigo Maul for their consultancy. Finally, and most importantly, I thank God for the accomplishment of this work.

REFERENCES

Anselmetti, F. S.; G. P. Eberli. 1993. Controls on sonic velocity in carbonates. Pure and Applied Geophysics, v. 141, no. 2–4, p. 287–323. https://doi.org/10.1007/BF00998333

Anselmetti, F. S.; G. P. Eberli. 1997. Sonic velocity in carbonate sediments and rocks. in I. Palaz and K. J. Marfurt, eds., Carbonate seismology: chapter 4. SEG Geophysical Developments Series, p. 53–74.https://doi.org/10.1190/1.9781560802099.ch4

Anselmetti, F.S.; Eberli G.P. 1999. The Velocity-Deviation Log: A tool to predict pore type permeability trends in carbonate drill holes from sonic and porosity or density logs. AAPG Bulletin, 83, 450-466. https:/doi.org/10.1306/00AA9BCE-1730-11D7-8645000102C1865D

Castro, D.D., Rocha, P.L.F. 2013. Quantitative parameters of pore types in carbonate rocks. Revista Brasileira de Geofísica, 31(1): 125-136. http://dx.doi.org/10.22564/rbgf.v31i1.251

Chang, H.K., Kowsmann, R.O., Figueiredo, A.M.F., Bender, A.A. 1992. Tectonics and stratigraphy of the East Brazil Rift System (EBRIS): an overview. Tectonophysics, 213, 97–138, https://doi.org/10.1016/0040-1951(92)90253-3.

Choquette, P.W. and Pray, L.C. 1970. Geologic Nomenclature and Classification of Porosity in Sedimentary Carbonates. American Association of Petroleum Geologists Bulletin, 54, 207-250. https://doi.org/10.1306/5D25C98B-16C1-11D7-8645000102C1865D

Faria, D.L., Reis, A.T. and Souza, O.G., Jr. 2017. Three-dimensional stratigraphic sedimentological forward modeling of an Aptian carbonate reservoir deposited during the sag stage in the Santos Basin, Brazil. Marine and Petroleum Geology, 88, 676–695, https://doi.org/10.1016/j.marpetgeo.2017.09.013

Garcia, S.F.M., Danderfer Filho, A., Lamotte, D.F. and Rudiewicz, J-L. 2012. Análise de volumes de sal em restauração estrutural: um exemplo na Bacia de Santos. Revista Brasileira de Geociências, 42, 433–450. 10.5327/Z0375-75362012000200016

Harahap, R. F., Riyanto, A., Haidar, M. W. 2020. Pore type-based carbonate reservoir characterization using rock physics modeling of “RF” field North Sumatera Basin. IOP Conference Series, The 4th Life and Environmental Sciences Academics Forum 2020, Indonesia, 846, 012015. doi:10.1088/1755-1315/846/1/012015

Kukla, P.A., Strozyk, F. and Mohriak, W.U. 2018. South Atlantic salt basins witnesses of complex passive margin evolution. Gondwana Research, 53, 41–57, https://doi.org/10.1016/j.gr.2017.03.012

Mann, J. and Rigg, J. 2012. New geological insights into the Santos Basin. GEOExPro, 9, 36–40

Maul, A., Cetale, M., Guizan, C., Corbett, P., Underhill, J. R., Teixeira, L., Pontes, R., González, M., 2021. The impact of heterogeneous salt velocity models on the gross rock volume estimation: an example from the Santos Basin pre-salt, Brazil. Petroleum Geoscience, https://doi.org/10.1144/petgeo2020-105.

Mavko, G., Mukerji, T., Dvorkin, J., 2009, The rock physics handbook: tools for seismic analysis of porous media, 2nd ed.: Cambridge University Press. https://doi.org/10.1017/CBO9780511626753

Moreira, J.L.P., Madeira, C.V., Gil, J.A. and Machado, M.A.P. 2007. Bacia de Santos. Boletim de Geociências da Petrobras, 15, 531–549

Ponte, F.C. and Asmus, A. H. 1978. Geological framework of the Brazilian continental margin. Geologische Rundschau, 67, 201–235, https://doi.org/10.1007/BF01803262

Quirk, D.G., Schødt, N., Lassen, B., Ings, S.J., Hsu, D., Hirsch, K.K. and Von Nicolai, C. 2012. Salt tectonics on passive margins: examples from Santos, Campos and Kwanza basins. Geological Society, London, Special Publications, 363, 207–244, https://doi.org/10.1144/SP363.10.

Saberi, R. M. 2013. Rock Physics Integration: From Petrophysics to Simulation 10th Biennial International Conference & Exposition. SPG, Kochi, Kerala, India. Paper id: P444.

Silva, E. P. A.; Davolio, A.; Santos, M. S.; Schiozer, D. J. 2017. Application of velocity-deviation log to predict the aspect ratio in Pre-Salt Carbonate rocks, 15th International Congress of the Brazilian Geophysical Society, SBGf, Rio de Janeiro, Brazil. https://doi.org/10.1190/sbgf2017-183

Silva, E.P.A.; Davolio, A.; Santos, M.S.; Schiozer, D.J. 2020. 4D petroelastic modeling based on a presalt well, Interpretation. 8, T639-T649.10.1190/INT-2019-0099.1

Wyllie, M.R.J., A.R. Gregory, and L.W. Gardner. 1956. Elastic wave velocities in heterogeneous and porous media. Geophysics, v. 21, no. 1, p. 41–70,1956. https://doi.org/10.1190/1.1438217

Xu, S.; Payne, M.A. 2009. Modeling elastic properties in carbonate rocks. The Leading Edge, 28, 66-74. https://doi.org/10.1190/1.3064148

Silva, E. P. A. da: lead; **Davolio, A.:** equal; **Santos, M. S. dos:** equal; **Schiozer, D. J.:** supporting.